Analysis of Common Rail Pressure Signal of Dual-Fuel Large Industrial Engine for Identification of Injection Duration of Pilot Diesel Injectors

Tomi Krogerus, **Mika Hyvönen** and **Kalevi Huhtala**

Tampere University of Technology, Laboratory of Automation and Hydraulic Engineering, Tampere, Finland

Email: tomi.krogerus@tut.fi

Phone: +358-50-3009077

Abstract

In this paper, we address the problem of identification of injection duration of common rail (CR) diesel pilot injectors of dual-fuel engines. In these pilot injectors, the injected volume is small and the repeatability of injections and identification of drifts of injectors are important factors, which need to be taken into account in order to achieve good repeatability (shot-to-shot with every cylinder) and therefore a well-balanced engine and furthermore reduced overall wear. This information can then be used for calibration and diagnostics purposes to guarantee engine longevity facilitated by consistent operating conditions throughout the life of the unit. A diagnostics method based on analysis of CR pressure with experimental results is presented in this paper. Using the developed method, the relative duration of injection events can be identified for multiple injectors. We use the phenomenon of drop in rail pressure due to an injection event as a feature of the injection process. The method is based on filtered CR pressure data during and after the injection event. First, the pressure signal during injection is extracted after control of each injection event. After that, the signal is normalized and filtered. Then a derivative of the filtered signal is calculated. Change in the derivative of the filtered signal larger than a predefined threshold indicates an injection event that can be detected and its relative duration can be identified. We present the experimental results and demonstrate the efficacy of the proposed methods using two different types of pressure sensors. We are able to properly identify a change of ≥ 10µs (2%, 500 µs) in injection time. This shows that the developed method detects drifts in injection duration and the magnitude of drift. This information can be used for adaptive control of injection duration, so that finally the injected fuel volume is the same as the original.

Keywords: analysis, dual-fuel engine, diesel, common rail, injector, rail pressure

1 Introduction

Recent technical and computational advances and environmental legislation have stimulated the development of more efficient and robust techniques for the diagnostics of diesel engines. Regulations concerning exhaust-gas emissions have also influenced the development of gas engines. To maintain a high compression ratio of the compression–ignition engine for higher overall engine efficiency, it is necessary to use a dual-fuel (gas-diesel) system.

Diesel engine fuel injection plays an important role in the development of combustion in the engine cylinder. The fuel injection process consists of periodic events from hundreds of microseconds to a few milliseconds, which need to be precisely controlled and continuously monitored in order to run smoothly. Arguably, the most influential component of the diesel engine is the fuel injection equipment: even minor faults can cause a major loss of efficiency of combustion and an increase in engine emissions and noise. The injection systems have been shown to be the largest contributing factor to diesel engine failure [1]. With increased sophistication (e.g. higher injection pressures) being required to meet continuously improving noise, exhaust smoke and gaseous emission regulations, the fuel injection equipment is becoming even more susceptible to failure.

Diagnostics of CR system and especially the diagnostics of CR injectors have been widely studied e.g. [2], [3], [4], [5], [6], [7], [8], [9], [10], [11], [12], [13]. Krogerus et al. [4] present a survey of the analysis, modelling, and diagnostics of diesel fuel injection systems. In this publication, typical diesel fuel injection systems and their common faults are presented. The most relevant state of the art research articles on diagnostics techniques and measured signals describing the behaviour of the system are reviewed and the results and findings are discussed. The increasing demand and effect of legislation related to diagnostics, especially on-board diagnostics (OBD), are discussed with reference to the future progress of this field.

Estimation of injected fuel amount has been studied in [5], [6], [7], [8]. Hoffmann et al. [5] have developed a model-based injection rate estimator, which takes into account the change in the injection behaviour due to wear and aging effects within the injector's nozzle. Extended Kalman filtering (EKF) was used in an observer scheme with the aim of accurately observing the injection rate by estimating the additional parameters of the fault model. Satkoski et al. [6], [7] summarize the development of a physics-based fuel flow estimator. Available measurements of piezo stack voltage and rail-to-injector line pressure are used for dynamic state estimation. Estimator results are compared against

both open-loop simulation and experimental data for a variety of profiles at different rail pressures, and show improvement, particularly, for more complex multi-pulse profiles. Bauer et al. [8] have developed a model for online estimation of fuel property parameters with the Unscented Kalman Filtering (UKF) method. The model was tested with data from a simulation model and a fuel injection system test rig that was specifically constructed for this purpose. It was found that it is possible to estimate the parameters with negligible bias and that the method is generally suitable.

Using the rail pressure signal for the diagnostics of injector events has been previously studied in [9], [10], [11] and [12]. Akiyama et al. [9] investigated a method to compensate the difference between an actual amount of injected fuel and a target one. In order to compensate the difference, the influence of pressure wave on fuel amount injected is investigated and injection period will be corrected is realized in an actual engine control system. Meanwhile, pressure wave propagation in common-rail was studied. Isermann et al. [6] developed a model-based fault detection module for CR injection systems. One of the simulated faults was a changed fuel volume through one of the injectors and it was realised by changing the desired injection quantity. The fault detection method was tested on an engine testbed with an Opel Z19 DTH four-cylinder CR diesel engine. By the simultaneous evaluation of several sensor signals, several symptoms in the form of deviations of calculated features can be generated. It was stated that by combining these symptoms and the symptoms calculated in the other fault detection modules and applying classification or inference methods several faults can be diagnosed. Payri et al. [11] studied injection diagnosis through CR pressure measurements, where the objective was to design an algorithm for isolation of the injection events. After the injection event, the rail pressure experiences a drop, which was used as a diagnostic feature of the injection process. Absence of such a drop when the ECU has commanded an injection signal would be a clear indication of a malfunction. Two different test benches were used, namely, a separate CR test bench and an engine test bench. Based on the experiments, the joint use of discrete Fourier transform (DFT) filter (referred to here as ideal filtering) and differentiation of the rail pressure signal seemed to be the best of the studied methods for detection of the injection events from the rail pressure measurement. It was stated that the method is useful even with small injections such as pilot injections. Marker et al. [12] studied the diagnostics of large light fuel oil (LFO) diesel engines where the main diesel injections were investigated. In this research the start and duration of injections are determined based on the pressure signal but each injector has an own pressure sensor close to each injector. This means that each injector incorporates an

accumulator with an upstream throttle. In addition, in this case, the injection event is easier to detect than the in case of pilot injections where the injected fuel amount is smaller and the effect on rail pressure is smaller. Of course, this is also rail specific, meaning the dimensions of the rail in use. In [12], filtering is used to attenuate the pressure oscillation, which is due to needle opening and closing events. When these are attenuated, the injection event can be analysed in more detail, in this case determining the injection duration. These frequencies of the pressure oscillations are rail specific.

Mancaruso et al. [13] have analysed pilot injection in a research diesel engine using non-conventional optical diagnostics. The visualization of the pilot injection process was obtained by means of an optical access in the piston head and by the presence of an inclined mirror for the collection of images. The aim of the work was to assess the potential and the suitability of infrared imaging for the investigation of the injection process.

According to the best knowledge of the writers, this is the first publication dedicated to the diagnostics of the CR diesel pilot injectors of dual-fuel large industrial engines using the rail pressure signal. The aim is to diagnose, meaning here to detect injection events and to identify the relative duration of the injection based on analysing the pressure signal of the CR in the case of changed injection duration, i.e. injected fuel volume, being changed for some reason e.g. degradation. The injected fuel volume of diesel pilot injectors is small and the repeatability of injections and identification of drifts of injectors is an important factor. The ultimate goal in our study is to use only one pressure sensor for the diagnostics of multiple pilot injectors e.g. 6 cylinder engines, although in this paper only one injector is presented. The rest of this paper is organised as follows. The next section presents the utilized CR test system including the studied injector. Then the diagnostics method is introduced followed by the experiments and the analysis results. Finally, the last section summarizes our conclusions.

2 Methodology

2.1 Experimental setup

The CR rail test system, a modified commercial CR system (passenger car), presented in Figure 1, was utilized to acquire measurement data for studying and developing of diagnostics methods. A second-generation pilot diesel injector of dual-fuel engine was installed to this test system. For this system, a custom-made electronic control unit (ECU) controlling the rail pressure of the CR system and the studied injector was made which made it possible to freely adjust the injection duration, number of injections, time between injections, control currents (boost and hold), pressure level etc. Castrol's diesel injector calibration oil 4113 [14] was used in the CR system.

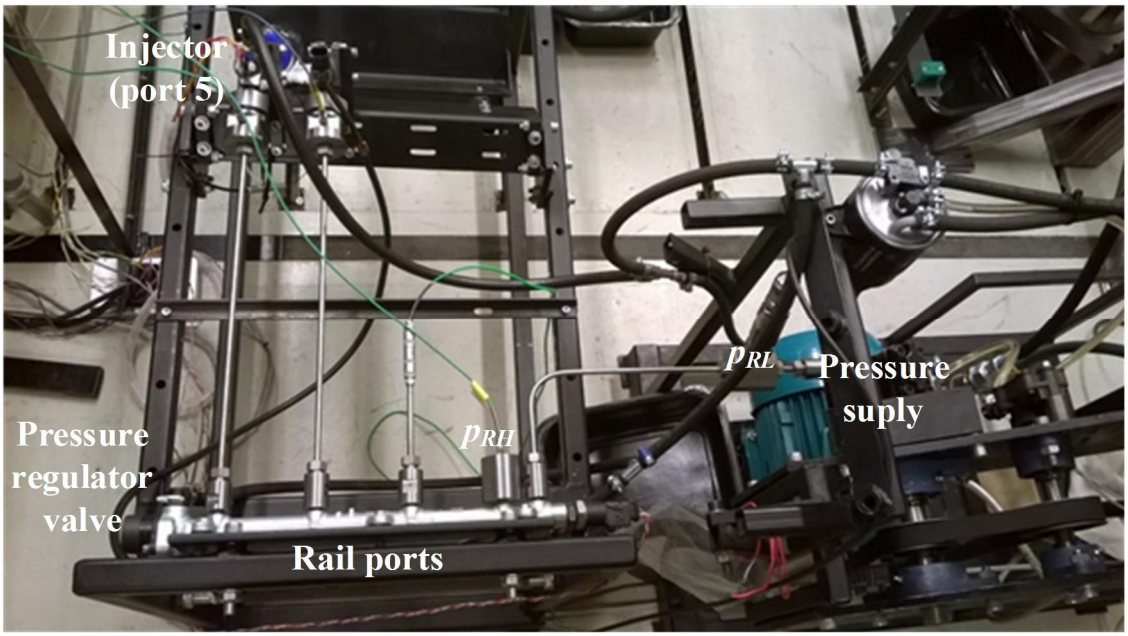

Figure 1. Experimental setup: CR test system.

The pressures of the CR system are measured using high dynamic Kistler pressure sensors (Type: 4067 A 2000), referred to here as p_{RH} and an accurate but lower dynamic Trafag sensor (EPN CR 20 A 1600 bar), referred to here as p_{RL}. A Bosch pressure sensor (original CR system sensor) is used for controlling the rail pressure level, and it is connected to the ECU. The studied injector includes a needle lift sensor (Micro-Epsilon eddyNCDT 3010), which enables accurate detection of needle opening and closing events. The control current of the injector and the pressure regulator were measured using LEM current transducer modules in the ECU. The temperatures were measured from the tank using a Pt100 sensor and from the rail using a K Type thermocouple. Figure 2 presents a schematic diagram of this CR system, including the installed sensors. The diagnostic method presented in this paper is based on the high dynamic pressure sensor p_{RH} but results are presented also with lower dynamic pressure sensor p_{RL}.

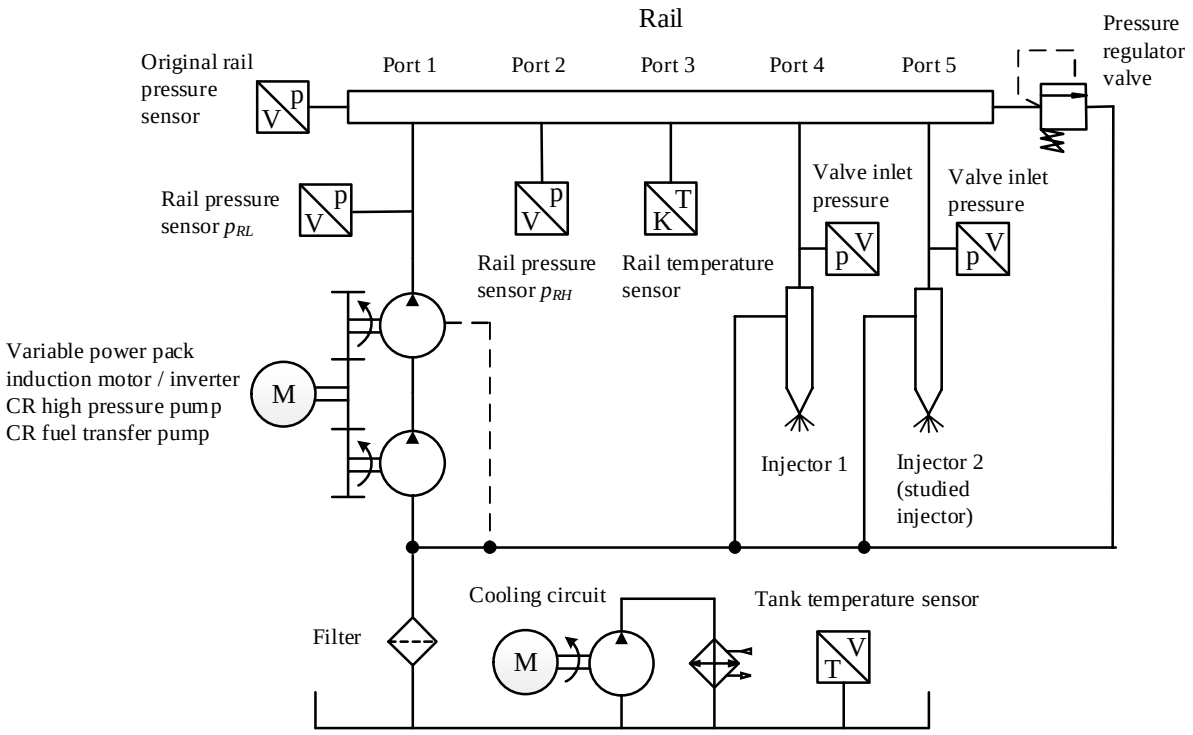

Figure 2. Schematic diagram of CR system including the installed sensors.

All the measurements were collected using a National Instruments data acquisition card type PCI 6125 using LabView software. The analysed rail pressure data (Kistler, p_{RH}) and the other rail pressure signal (Trafag, p_{RL}), injection current and needle lift were sampled at 250 kHz frequency. The Kistler pressure sensor is suitable for measuring static and high dynamic pressures while the Trafag pressure sensor is meant for measuring static measurements. Therefore, Kistler sensor p_{RH} was primarily utilised for analysis purposes. Due to the limitations of the used acquisition card (max. 1 MHz) injector input pressure and temperatures were not collected. Temperatures were collected manually. Original rail pressure and pressure regulator control current were used in ECU but were not recorded.

The analysis of the rail pressure signals was made using Mathworks' Matlab software. Matlab's Signal Processing Toolbox is used in designing implementation of filtering where rest of the algorithm is self-implemented.

2.2 Mathematical description of flow dynamics

In the high-pressure CR system the fast opening and closing of the injector needle will cause high-amplitude, high-frequency fluid transients. Understanding the behaviour of the propagation of the pressure wave in the system is essential when analysing the measured pressure data of the system. When a pressure wave is propagated through a common rail circuit, the wave emitted from one injector can also affect other injectors and pipelines of the CR system. It is important to understand this when analysing the operation of the complete CR

system and in the development of diagnostics methods for it.

The physics of the fluid flow consist of a composition of conservation mass, momentum and energy. Three widely discussed Navier-Stokes differential equations [15] are: continuity equation,

$$\frac{\partial \rho}{\partial t} + \frac{\partial(\rho \cdot u)}{\partial x} + \frac{\partial(\rho \cdot v)}{\partial y} + \frac{\partial(\rho \cdot w)}{\partial w} = 0 \quad (1)$$

momentum equation,

$$\rho \cdot V \cdot \frac{Du}{Dt} = \sum F \quad (2)$$

and conservation of energy which defines the fluid flow in the piping and injector [16],

$$\Delta m \cdot \frac{D}{Dt}\left(e + \frac{1}{2} \cdot \vec{c}^{\,2}\right) = P + Q \quad (3)$$

where ρ is fluid density, t is time, x, y, z are Cartesian coordinates and u, v and w velocity components respectively, V is volume and F is force, e is specific internal energy, $\vec{c}$ is velocity vector, P is mechanical power and Q is heat flux.

In a high-pressure common rail system with fast and high-amplitude fluid transients, the inertial effects of the fluid will be more dominant than in the analysis of conventional hydraulic systems. There are two different approaches for understanding the fluid transients in CR systems. The first consists of frequency domain methods, mostly targeted on linear analysis in steady state conditions. The other approach focuses on time domain methods, which are more suitable for explaining and understanding, for example the water hammer effect happening in rapid fluid flow transients caused by fast opening and closing of the injector needle. In [17] a commonly used method widely used today is discussed.

Nowadays the most common methods are finite element methods (FEM) or finite volume methods (FVM) and several commercial and open source software are available for modelling, analysing and understanding the dynamics of the fluid flow under rapid transients. These software are beneficial when developing tools for understanding the pressure oscillations of complete, often also quite complex, CR systems.

The real CR system includes several injectors, a high-pressure pump, pressure regulating valve and other components, which can cause pressure oscillations to the fluid flow even at a distance from the original source. Therefore filtering is needed to separate different flow transient sources from each other and to attenuate the pressure oscillation, which are due to needle opening and closing events. When these are attenuated the injection event can be analysed in more detail, in this case to determine the injection duration. The frequencies of the pressure oscillations are rail specific. The natural frequency of the rail is defined as

$$f_r = \frac{2}{c_s * l_r} \quad (4)$$

where c_s is the speed of sound in diesel fuel and l_r is the length of the rail. Figure 3 presents examples of this phenomenon in the studied rail with injection times of 500 µs to 6 ms. With different injection

times the pressure oscillation either strengthens or attenuates. Figures 4 and 5 present how the frequency of the pressure oscillation is also pressure dependent. Figure 4 presents an injection duration of 500 µs with four different pressure levels: 500 bar, 900 bar, 1200 bar and 1400 bar. Figure 5 presents FFT transforms of these where we can see how the oscillation frequency increases with the pressure. From here we can deduce the frequency level to be used with low-pass filtering to attenuate the interfering oscillation.

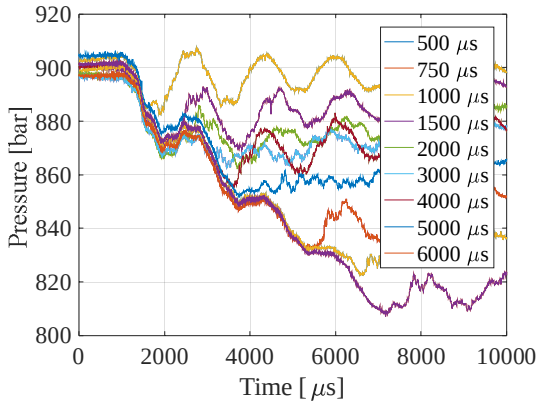

Figure 3. Oscillation of rail pressure signal due to needle opening and closing with injection times of: 500 µs, 750 µs, 1000 µs, 1500 µs, 2000 µs, 3000 µs, 4000 µs, 5000 µs and 6000 µs.

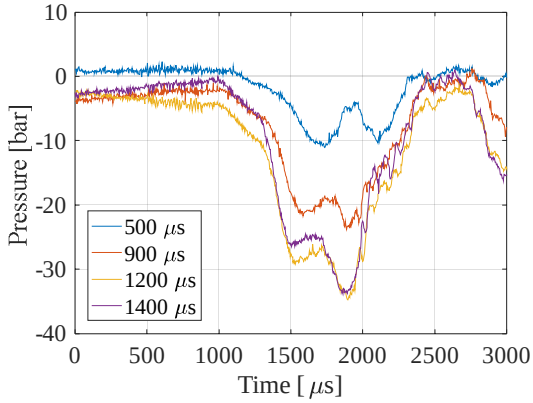

Figure 4. Pressure drop due to injection with injection pressures of: 500 bar, 900 bar, 1200 bar and 1400 bar.

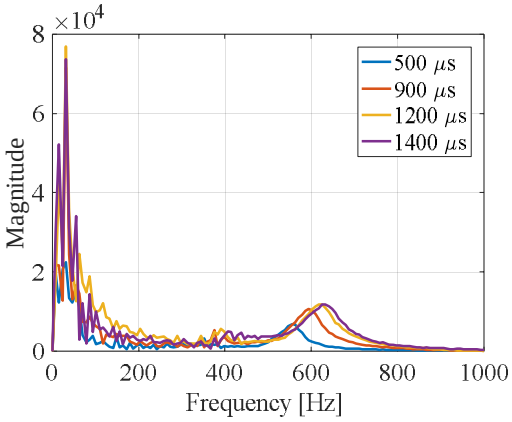

Figure 5. Frequency domain representation of rail pressure using Fast Fourier Transform.

Figure 6 presents the measured and simulated pressure curves of the CR system of the 6-cylinder engine with an injection timing order of 2-4-1-5-3-6. In the simulated data, auxiliary components such as high-pressure fuel pump and pressure regulator valve are not modelled. The simulation model of the CR system is made using GT-SUITE software and is based on [15] and [18]. The model takes into account equations (1), (2) and (3) for 1D fluid flow. The model of a single injector is verified using experimental measurements from CR test system (see Fig. 1 and 2). The complete simulation model with six cylinders was not possible to verify accurately with the measurement data from a real engine, because only few measurements were available. However, similarities can be seen when comparing measurements and simulations, especially in the beginning of every injection. Simulation of the CR system is performed to increase understanding of the pressure oscillation phenomena. The model also gives information about the timing of each cylinder, which are marked with

a green circle in Fig. 6. The pressures presented in Fig. 6 are measured from the beginning of the rail. The data in Fig. 6 clearly highlights the differences in pressure oscillations in a real CR system and it is important that this is taken into account when developing diagnostics methods for real CR systems. It can be clearly seen from Fig. 6 that the pressure oscillation in the measurement and simulation is different for the injection of all the cylinders. This is related to the volume flow dynamics and pressure wave propagation in the CR system pipeline. The highest amplitudes can be seen coming from cylinders 1 and 6, both located at the end of the rail, and lowest for the cylinders in the middle of the rail. A common feature for all cylinders is the sudden pressure drop right after the injection event, with the exact time depending on the distance of the pipeline between measurement and injector nozzle.

The diagnostic method presented in this paper can be utilised for real CR systems with multiple cylinders and injectors when the parameters of the developed diagnostics method, i.e. separate filtering frequencies and delays, are selected individually for each injector. As was previously stated, this is due to the different pipeline distance between measurement and injector nozzle.

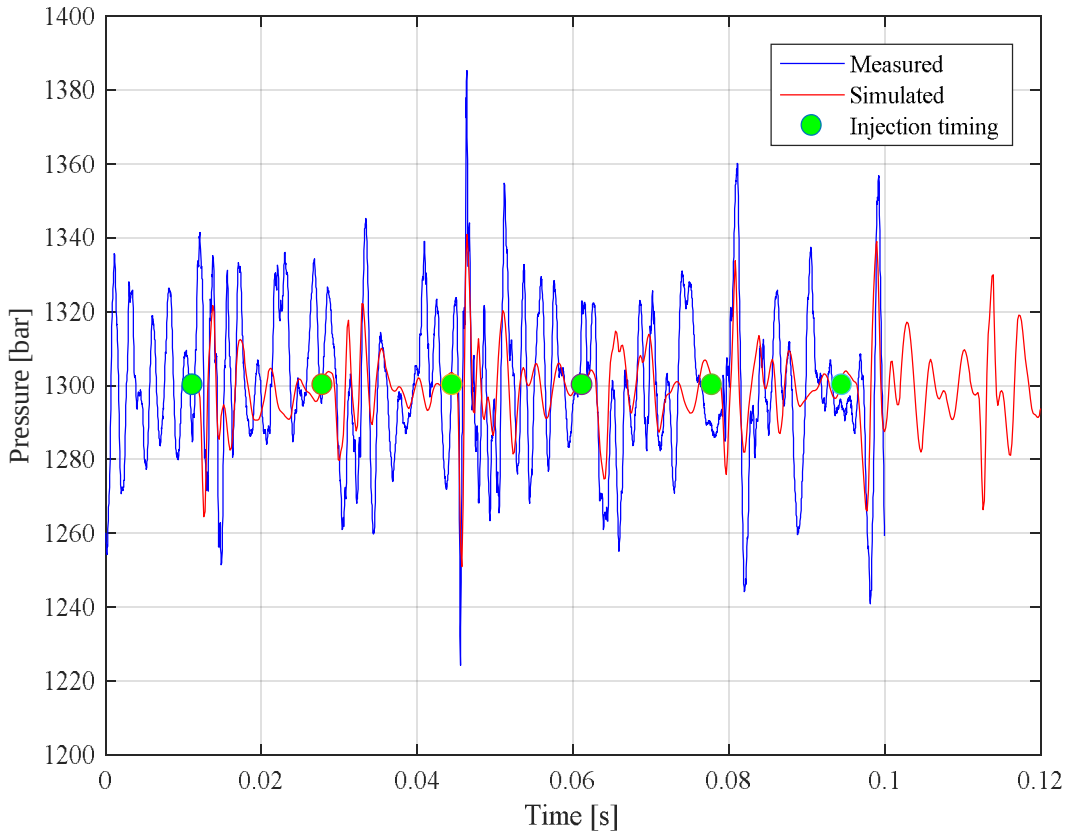

Figure 6. Simulation of rail pressure in the case of a 6 cylinder engine.

2.3 Diagnostics method

The analysed rail pressure is feedback controlled by the pressure regulator valve (see: Figure 2). With every injection, fuel from the rail is injected into the cylinder through the injector thus the rail pressure suddenly drops (see Figures 3, 4 and 7) and we use this phenomenon as a feature, as a fingerprint, of injection, and its pattern after filtering is used to identify the duration of the injections.

Using this analysed information, namely the start and duration of injection, adaptive control of injection and as-new performance can be achieved.

Figure 7 presents a typical pressure drop with oscillations due to injection and corresponding control current of the injector. Besides these, an example of six injections corresponding to approx. 720 degree crank angle (ºCA) of an engine is presented. It should be noted here that approx. 10 ms of data is collected after each injection (see: Figure 7 the lowest figure) while using the control current signal to trigger the data acquisition.

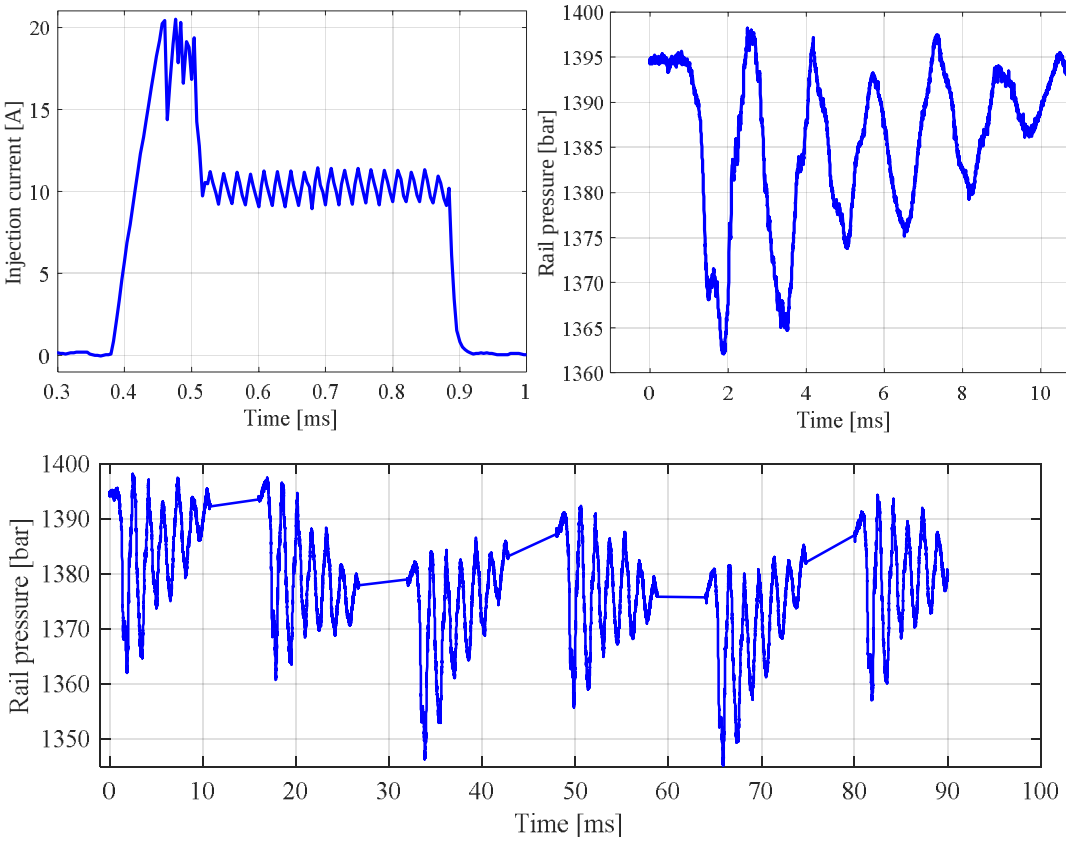

Figure 7. Example of injector current, rail pressure after single injection and six injections (720 ºCA) with 16ms time between injections.

In the method, the pressure signals during the injection are first extracted after control of each injection event. To this effect, we let $x(t): t \in \{0, \dots, t_f\}$, where t_f is the final time point, to represent the pressure signal during 720 degree crank angle (ºCA) of an engine and $x_i(t): t \in \{t_{s_i}, \dots, t_{e_i}\}$ for $i = 1, \dots, M$ represent the extracted data signals sampled with constant sampling frequency; *M* is the number of injection events and t_{s_i} the start time of an injection *i* and respectively t_{e_i} is the end time of an injection *i*.

Thus, we sample the constant number of samples in the case of each injection event; $x_i(n): n \in \{1, \dots, N\}$, where N is the number of data points sampled. After that, the signal is normalized by scaling it to zero mean and unit variance. This is done by removing the mean and dividing the result by its standard deviation

$$x_z(n) = x_i(n) - \bar{x} \quad (5)$$

where $\bar{x} = \frac{1}{N}\sum_{n=1}^{N} x_i(n)$ and N is the number of data points in signal x_i

$$x_n(n) = \frac{x_z(n)}{x_s} \quad (6)$$

where $x_s = \sqrt{\frac{1}{N-1}\sum_{n=1}^{N}(x_i(n) - \bar{x})^2}$

After this offset is reset

$$x_r(n) = x_n(n) - x_n(t_c) \quad (7)$$

where t_c is the time instance when the control of injector is activated. Resetting the offset means removing pressure level difference between single injections. This is due to the phase of the axial piston pump not being the same in each data set because the series of injections is started manually. In real engines, this has been taken into account and offset resetting is not needed. Another option would be to remove the trend (pressure oscillation due to pump) and fit a low order polynomial to the signal and then use the polynomial to detrend it.

After offset reset, the signal $x_r(n)$ is filtered using a 10th order lowpass IIR Butterworth filter with cut-off frequency of 450 Hz to attenuate the pressure oscillations. The cutoff frequency is the frequency at which the magnitude response is 3 dB below the passband gain. The primary advantage of IIR filters over FIR filters is that they typically meet a given set of specifications with a much lower filter order than a corresponding FIR filter. If implemented in a signal processor, this implies a correspondingly lower number of calculations per time step; the computational savings are often of a rather large factor. This means that IIR filters can achieve a given filtering characteristic using less memory and calculations than a similar FIR filter. Although IIR filters have a nonlinear phase, data processing is performed when the entire data sequence is available prior to filtering. This allows for a non-causal, zero-phase filtering approach, which eliminates the nonlinear phase distortion of an IIR filter. In the case of real engine and multiple injectors, a separate cut-off frequency for each injector is needed.

Transfer function of IIR filter is defined according to Eq. 8. Considering that in most IIR filter designs coefficient a_0 is 1, the IIR filter transfer function takes the more traditional form.

$$H(z) = \frac{Y(z)}{X(z)} \quad (8)$$

$$= \frac{\sum_{k=0}^{P} b_k z^{-k}}{1 - \sum_{l=1}^{Q} a_l z^{-l}}$$

$$= \frac{b_0 + b_1 z^{-1} + \cdots + b_P z^{-P}}{1 - a_1 z^{-1} - \cdots - a_Q z^{-Q}}$$

The coefficients of the numerator polynomial, denoted as $B(z)$, correspond to the feed-forward terms of the difference equation. The coefficients of the denominator polynomial, denoted as $A(z)$, for z^{-l}, $l > 0$ correspond to the feedback terms of the difference equation. IIR filters have feedback (a recursive part of a filter) and are therefore known as recursive digital filters therefore. Coefficients can be derived from Eq. 8, and using the condensed form of the difference equation, the filtered signal can be expressed as follows

$$y_f(n) = \sum_{k=0}^{F} b_k x_r(n-k) - \sum_{k=1}^{F} a_k y_f(n-k) \quad (9)$$

where F is the feedforward and feedback filter order, b_k are the feedforward filter coefficients, a_k the feedback filter coefficients, $x_r(n)$ the input signal and $y_f(n)$ is the output signal.

After filtering, a derivative of the filtered signal is calculated

$$y_d(n) = y_f(n) - y_f(n-1) \quad (10)$$

Change in the derivative of the filtered signal $y_d(n)$ smaller than a predefined threshold thr indicates an injection event and the start of injection

$$n_{SoI} = n, \quad (11)$$
$$y_d(n-1) > thr \geq y_d(n) : n \in \{1, \dots, N\}$$

Similarly, after the detected start of injection, change in the derivative of the filtered signal $y_d(n)$ larger than a predefined threshold thr indicates the end of injection

$$n_{EoI} = n, \quad (12)$$
$$y_d(n-1) < thr \leq y_d(n) : n \in \{n_{SoI} + 1, \dots, N\}$$

Using the corresponding identified relative start time t_{SoI} and end time t_{EoI} of injection, the relative duration of injection t_{RDoI} can be calculated

$$t_{RSoI} = n_{SoI} T \quad (13)$$

$$t_{REoI} = n_{EoI} T \quad (14)$$

$$t_{RDoI} = t_{REoI} - t_{RSoI} \quad (15)$$

where T is the sample time.

3 Results and discussion

The developed method was validated using the CR test system with one injector (see: Figures 1 and 2). In the experiments, the system was first warmed to 37 °C by driving test cycles with high pressure and a thermostat controlled cooling system maintains the temperature at 37 ± 1°C.

Table 1. Experiments.

Pressure level [bar]	Injection time [µs]	Number of injections	Time between injections [µs]	Rotational speed [rpm]	Temperature [°C]
1400	500	100	16	600	37.6
1400	505	100	16	600	37.0
1400	510	100	16	600	36.9
1400	525	100	16	600	36.8
1400	550	100	16	600	36.8
1400	600	100	16	600	36.7
1400	750	100	16	600	36.7

Injection times of 500µs, 505µs, 510µs, 525µs, 550µs, 600µs and 750µs (an increase of 1, 2, 5, 10, 25 and 50 % in this injection time) were used to simulate a drift of injection duration, see Table 1.

The time between injections was 16 ms (approx. 6 injections per 720 ºCA). The pressure level was 1400 bar. One hundred injections per different injection time were used, so altogether 700 injection events were analysed. The sampling frequency of the measurements was 250 kHz. This high sampling frequency is not needed but still it needs to be ≥ 10 kHz, and preferably closer to 30 kHz to enable high enough resolution to achieve good repeatability for every injection and therefore well balanced engine.

In the analysis, the pressure signal during the injection is first extracted (see Fig. 8a). After that, the signal is normalized and offset is reset (see Figure 8b). After removing the offset, the signal is filtered (see Fig. 8c). Then a derivative of the filtered signal is calculated (see Fig. 8d). Here, $thr = -1.5$.

In Fig. 8d, the mean values of 100 injections for different injection times are presented. Here it can be noticed that a ≥ 2% change (= 10µs) in injection time can be identified.

The method was tested also using the other low dynamics pressure sensor (p_{RL}). Figure 9 presents the extracted and derived filtered pressure signals (p_{RL}). Here, $thr = -1.0$. Surprisingly good results were obtained also using this pressure sensor although that it does not correctly represent the dynamic changes of pressure after the injection event. The data of this sensor contain more noise (see Fig. 9a) and need to be removed using e.g. median filter (used here) before offset resetting and low-pass filtering. The challenge with this kind of sensor is that the region for setting the threshold for identification of relative duration of injections is quite narrow and some injections might be excluded from analysis due to this.

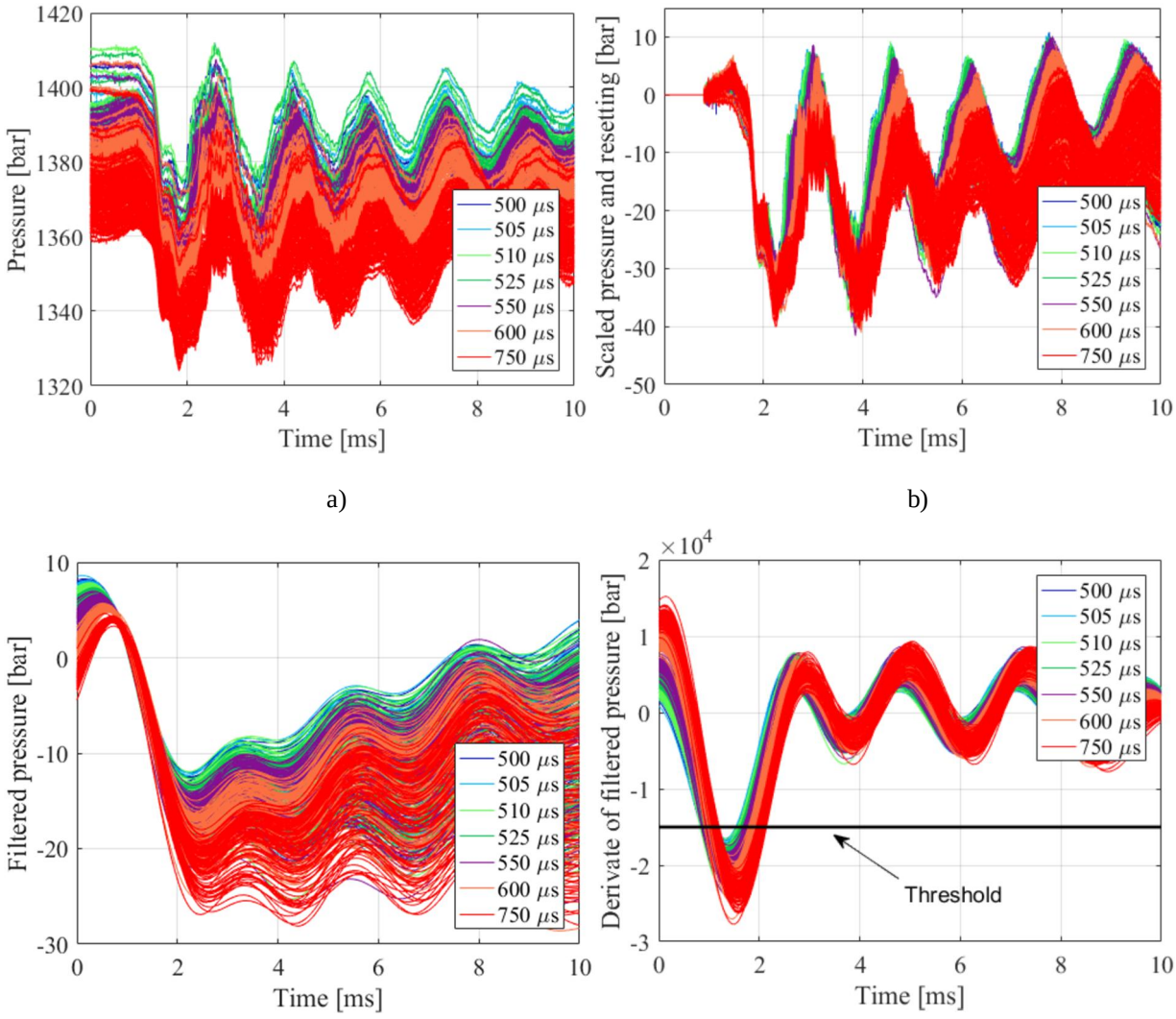

Figure 8. a) extracted, b) normalized and offset reset, c) filtered, d) derivative of filtered pressure signals (p_{RH}) with threshold.

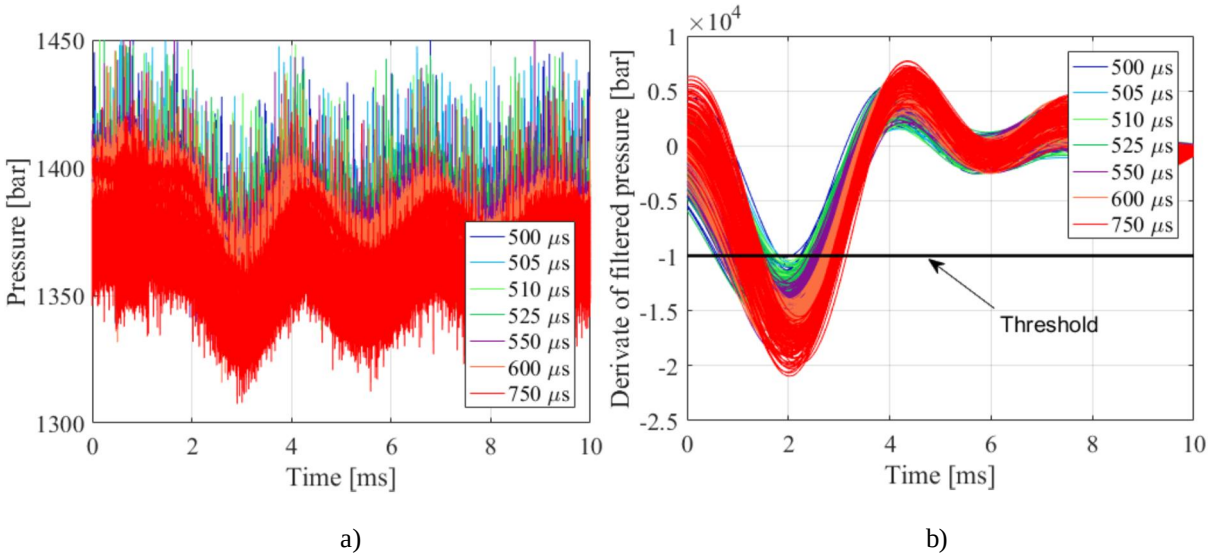

Figure 9. a) extracted pressure signals and b) derivative of filtered pressure signals (p_{RL}) with threshold.

Figures 10 present the mean of the identified relative injection duration (t_{RDoI}) of 100 injections for different injection times with both sensor types (p_{RH} and p_{RL}) . It is possible to fit a curve to these values and calculate the real injection duration. Change with p_{RH} sensor is more linear than with p_{RL} sensor: see Fig. 10. Here can be noticed that a ≥ 2% change (= 10µs, p_{RH}) in injection time can be identified. Here it should be noted that the detected increase in duration is due to the increased value of t_{EoI} while the values of t_{SoI} are relatively close to each other as could be expected. To compensate for this drift the time t_{EoI} should be smaller.

Figures 11 show all the identified t_{RDoI} values (500µs and 750µs). It can be seen that the identified t_{RDoI} values have quite large deviation but the trend can be easily seen and should be used instead of single identified values. Most of this deviation is supposed to result from pressure level change due to axial piston pump even though some of its effect is removed in offset resetting. As was stated earlier, this is supposed to be reduced in the case of a real engine where single injection events are always in the same phase with the axial piston pump.

Figures 12 present the percentage change of identified t_{RDoI} as a function of injection time. Figures 13 present the standard deviation of the identified t_{RDoI}. As could be expected, the deviation of the results becomes smaller when the injection time increases, and the operation of the injector from shot-to-shot becomes more robust. Additionally, it should be noticed that the relative standard deviation of the p_{RL} sensor is much higher than p_{RH}. Therefore, the repeatability is better using the p_{RH} sensor.

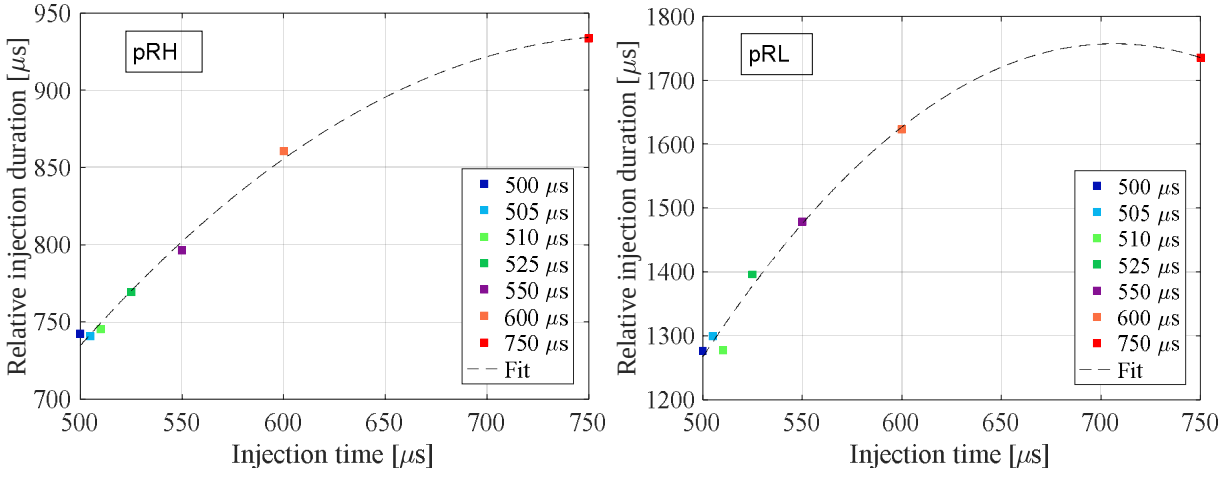

a) b)

Figure 10. a) mean of t_{RDoI} and fitted 2nd order polynomial with p_{RH}, b) mean of t_{RDoI} and fitted 2nd order polynomial with p_{RL}.

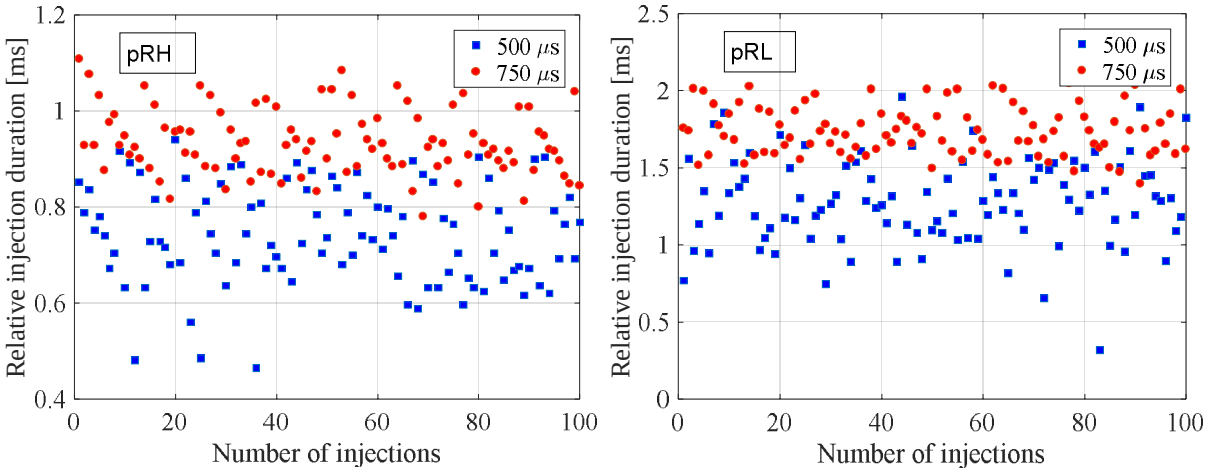

a) b)

Figure 11. a) identified t_{RDoI} with p_{RH}, b) identified t_{RDoI} with p_{RL}.

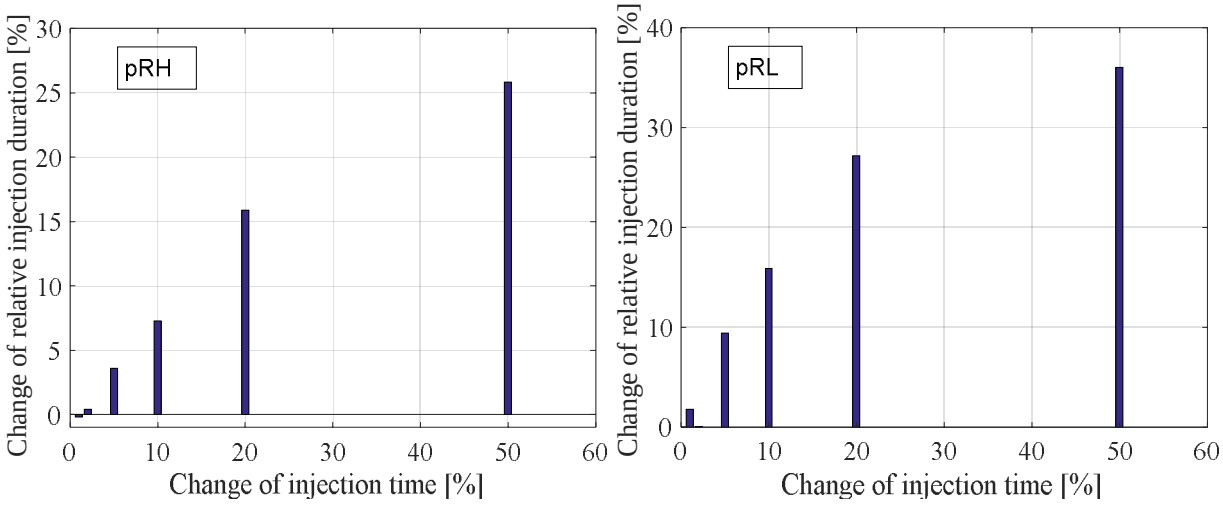

a) b)

Figure 12. a) percentage change of t_{RDoI} as a function of injection time with p_{RH}, b) percentage change of t_{RDoI} as a function of injection time with p_{RL}.

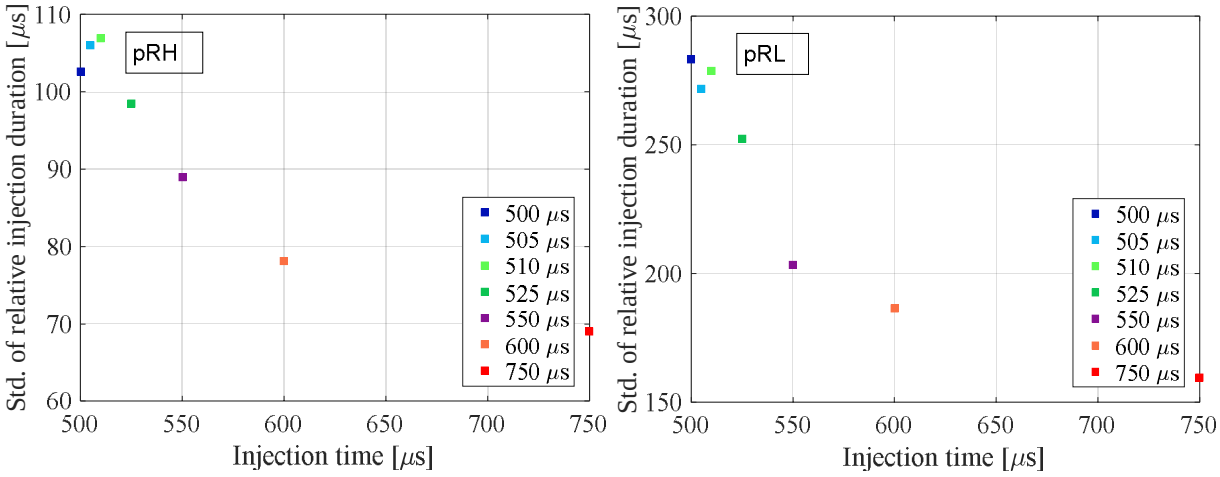

a) b)

Figure 13. a) standard deviation of t_{RDoI} with p_{RH}, b) standard deviation of t_{RDoI} with p_{RL}.

The actual injection duration can be calculated by fitting a curve to the results of the relative duration. As an example, a fitted second order polynomial is presented in Figure 10. It describes the data reasonable well. This part has not been studied in more detail and should be addressed in possible further studies. This means, examining the error made in calculation of an actual injection time using the fitted model.

4 Conclusions

Analysis of the common rail pressure signal of a dual-fuel large industrial engine for identification of injection duration of pilot diesel injectors was presented in this paper. A method based on analysis of drop of the CR rail pressure after injection event was presented with experimental results using a single injector. Two different pressure sensors (p_{RH} and p_{RL}) were utilized to study the relative duration of injection. Injection times of 500µs - 750µs (an increase of 1, 2, 5, 10, 25 and 50 % in this injection time) were used to simulate a drift of injection duration. This changed injection time was detected and its relative duration was calculated from the rail pressure signal. The experimental results show that the developed method detects drifts of injection duration and identifies the magnitude of drift, which can be used for adaptive control of injection duration. The results show that changes of ≥ 10 µs (2%, 500 µs) in injection time can be properly identified using a high dynamic pressure sensor (p_{RH}). In addition, surprisingly good results were also obtained using a low dynamic pressure sensor (p_{RL}) although that it does not correctly represent the dynamic changes of pressure after the injection event. Changes of ≥ 25 µs (5%, 550 µs) in injection time can be identified using this low dynamics (p_{RL}), sensor but it should be noted that some injection cases were omitted from analysis due to challenges in adjusting the threshold, and standard deviation is also much higher than with a high dynamics sensor

(p_{RH}). The authors believe that the results are better with high dynamic pressure sensor (p_{RH}) as it represents dynamic changes of pressure better after the injection event and low dynamic sensor data needs pre-filtering, e.g. median filtering, before further analysis. These things together create the difference in results between the sensor types.

In the case of multiple injectors in a real engine the diagnostics parameters of each injector need to be defined separately. Consequently, reference models of relative injection duration need to be trained for all the injection cases in the engine map.

Acknowledgements

The authors gratefully acknowledge the support of this work by DIMECC's (The Strategic Centres for Science, Technology and Innovation) S-STEP Program, Smart Technologies for Lifecycle Performance.

References

1 Gill, J., Reuben, R., Steel, J., Scaife, M., and Asquith, J. A Study of Small HSDI Diesel Engine Fuel Injection Equipment Faults Using Acoustic Emission. Journal of Acousic. Emission 2000;18:211–216.

2 Mohammadpour, J., Franchek, M., and Grigoriadis, K. A Survey on Diagnostics Methods for Automotive Engines. International Journal of Engine Research 2011;13:41–64.

3 Jones, N., Li., Y. A Review of Condition Monitoring and Fault Diagnosis for Diesel Engines. Tribotest 2000;6:267–291.

4 Krogerus, T., Hyvönen, M., Huhtala, K. A Survey of Analysis, Modeling,and Diagnostics of Diesel Fuel Injection Systems. Journal of Engineering for Gas Turbines and Power: Transaction of the ASME 2016;138:1-11.

5 Hoffmann, O., Han, S. and Rixen, D. Common Rail Diesel Injectors with Nozzle Wear: Modeling and State Estimation. SAE Technical Paper 2017-01-0543.

6 Satkoski, C., Ruikar, N., Biggs, S. and Shaver, G. Cycle-to-cycle Estimation and Control of Multiple Pulse Profiles for a Piezoelectric Fuel Injector. Proceedings of the 2011 American Control Conference on O'Farrell Street. San Francisco, CA, USA, June 29 - July 01, 2011, 965-972.

7 Satkoski,C. and Shaver, G. Piezoelectric Fuel Injection: Pulse-to-Pulse Coupling and Flow Rate Estimation. IEEE/ASME Transaction on Mechatronics 2011;16:627-642.

8 Baur, R., Zhao, Q., Blath, J., Kallage, F., Schultalbers, M. and Bohn, C. Estimation of Fuel Properties in a Common Rail Injection System by Unscented Kalman Filtering. Proceedings of the IEEE Conference on Control Applications (CCA). Antibes, France, October 8-10, 2014, 2040-2047.

9 Akiyama, H., Yuasa, H., Kato, A., Saiki, T. et al. Precise Fuel Control of Diesel Common-Rail System by Using OFEM. SAE Technical Paper 2010-01-0876, 2010.

10 Isermann, R., Clever, S. Model-Based Fault Detection and Diagnosis for Common-Rail Injections Systems. MTZ 2010;22:344–349.

11 Payri, F., Luján, J., Guardiola, C., Rizzoni, G. Injection Diagnosis Through Common-Rail Pressure Measurement. Proceedings of the Mechanical Engineering, Part D: Journal of Automobile Engineering 2006;220:347-357.

12 Marker, J., Willmann, M. Potential of INSITU closed-loop control of fuel injection in large LFO engines. Proceedings of the 15th Conference of the Working Process of the Internal Combustion Engine. Graz, Austria, September 24-25, 2015, 393-402.

13 Mancaruso, E., Sequino, L., and Vaglieco, B. Analysis of the Pilot Injection Running Common Rail Strategies in a Research Diesel Engine by Means of Infrared Diagnostics and 1D Model. Fuel 2016;178:188–201.

14 Castrol Limited. Castrol diesel injector calibration oil 4113. Last accessed April 10, 2017.

http://msdspds.castrol.com/bpglis/FusionPDS.nsf/Files/2AF8D13D25BFB750802577E0005BB19F/$File/BPXE-8BGMVA_0.pdf

15 Beierer, P. Experimental and Numerical Analysis of the Hydraulic Circuit of a High Pressure Common Rail Diesel Fuel Injection System. Department of Intelligent Hydraulics and Automation, Tampere University of Technology; 2008. PhD thesis.

16 Anderson, D. Computational Fluid Dynamics. New York: McGraw-Hill, Inc.; 1995.

17 Taylor, S., Johnston D. and Longmore, D. Modelling of Transient Flow in Hydraulic Pipelines. Proceedings of the Institution of Mechanical Engineers, Part I: Journal of Systems and Control Engineering, 1997;211:447–455.

18 Payri, R., Salvador, F., Martí-Aldaraví, P. and Martínez-López. Using One-Dimensional Modelling to Analyse the Influence of the Use of Biodiesels on the Dynamic Behaviour of Solenoid-Operated Injectors in Common Rail Systems: Detailed Injection System Model. Energy Conversion and Management 2012;54:90-99.